Innate immunity and transcription of MGAT-III and Toll-like receptors in Alzheimer's disease patients are improved by bisdemethoxycurcumin

Milan Fiala*†, Philip T. Liu‡, Araceli Espinosa-Jeffrey§, Mark J. Rosenthal*, George Bernard§¶, John M. Ringman‖, James Sayre**, Laura Zhang*, Justin Zaghi*, Sheila Dejbakhsh*, Ben Chiang*, James Hui*, Michelle Mahanian*, Anita Baghaee*, Pamela Hong*, and John Cashman††

*Department of Medicine, Greater Los Angeles Veteran's Affairs Medical Center, and Departments of ‡Medicine, Microbiology, Immunology and Molecular Genetics, §Neurobiology, and ‖Neurology, University of California School of Medicine, Los Angeles, CA 90095; ¶Division of Oral Biology, University of California School of Dentistry, Los Angeles, CA 90095; **Department of Biostatistics, University of California School of Public Health, Los Angeles, CA 90095; and ††Human BioMolecular Research Institute, San Diego, CA 02121

Edited by Louis J. Ignarro, University of California School of Medicine, Los Angeles, CA, and approved June 15, 2007 (received for review February 15, 2007)

We have tested a hypothesis that the natural product curcuminoids, which has epidemiologic and experimental rationale for use in AD, may improve the innate immune system and increase amyloid-β (Aβ) clearance from the brain of patients with sporadic Alzheimer's disease (AD). Macrophages of a majority of AD patients do not transport Aβ into endosomes and lysosomes, and AD monocytes do not efficiently clear Aβ from the sections of AD brain, although they phagocytize bacteria. In contrast, macrophages of normal subjects transport Aβ to endosomes and lysosomes, and monocytes of these subjects clear Aβ in AD brain sections. Upon Aβ stimulation, mononuclear cells of normal subjects up-regulate the transcription of β-1,4-mannosyl-glycoprotein 4-β-*N*-acetylglucosaminyltransferase (*MGAT3*) ($P < 0.001$) and other genes, including Toll like receptors (*TLRs*), whereas mononuclear cells of AD patients generally down-regulate these genes. Defective phagocytosis of Aβ may be related to down-regulation of *MGAT3*, as suggested by inhibition of phagocytosis by using *MGAT3* siRNA and correlation analysis. Transcription of *TLR3*, bditTLR4, *TLR5*, bditTLR7, *TLR8*, *TLR9*, and *TLR10* upon Aβ stimulation is severely depressed in mononuclear cells of AD patients in comparison to those of control subjects. In mononuclear cells of some AD patients, the curcuminoid compound bisdemethoxycurcumin may enhance defective phagocytosis of Aβ, the transcription of *MGAT3* and TLRs, and the translation of TLR2–4. Thus, bisdemethoxycurcumin may correct immune defects of AD patients and provide a previously uncharacterized approach to AD immunotherapy.

amyloid-β | phagocytosis | endocytosis | MGAT3 siRNA

According to the amyloid-β (Aβ) hypothesis, amyloidosis occurring in the brain of patients with Alzheimer's disease (AD) by fibrillar Aβ 1–42 and 1–40 (1) and Aβ oligomers (2) is a leading cause of neurodegeneration in AD (3). Macrophages and microglia are the innate immune cells responsible for clearance of pathogens and waste products. We have shown that blood-borne monocyte/macrophages of AD patients migrate across the blood–brain barrier into AD brain but are defective in clearance of Aβ in neuritic plaques (4), and they overexpress cyclooxygenase-2 and inducible NO synthase (4). Resident microglia in AD brain display markers of inflammation (5, 6), phagocytosis (7), and proinflammatory but not prophagocytic genes (8). However, most microglia invading Aβ plaques in transgenic mouse models are bone marrow-derived, not resident microglia (9). Thus, the brains of AD patients and transgenic mice seem to display inflammatory responses by microglia and defective Aβ clearance by blood-borne macrophages. Consequently, the defective innate immune system of AD patients might be a culprit in brain amyloidosis leading to brain inflammation.

The mechanisms of neurodegeneration produced by abnormally folded proteins, Aβ, and phosphorylated τ remain an enigma (10). The pathogenesis of neurodegeneration in AD involves the impact of polymorphic proteins, such as amyloid precursor protein (APP), apolipoprotein E (11, 12), sortilin-related receptor, low-density lipoprotein receptor class A repeat-containing protein (SORL1) (13), reelin (14), interleukin 1, α1-antichymotrypsin, and α2-macroglobulin (15, 16) on cellular processes, such as APP processing (13), oxidative stress (17, 18), and neuronal apoptosis (19–21). However, Aβ accumulation is considered the major mechanism susceptible to therapy (22).

To clarify the role of the innate immune system in brain amyloidosis, we investigated Aβ phagocytosis and transcriptional regulation by macrophages and peripheral blood mononuclear cells (PBMCs) of AD patients and controls. In addition, we tested immune modulation of Aβ phagocytosis and gene transcription and translation by treatment with the compound bisdemethoxycurcumin derived from curcuminoids.

Results

Transcriptional Down-Regulation of *MGAT3* and Other Genes in PBMCs of AD Patients. In the initial study using the Operon platform, we performed microarray analysis of mRNAs isolated from PBMCs of two patients and two controls. Compared with AD cells, after overnight treatment with Aβ, control cells up-regulated (>2.2-fold) the transcription of 35 genes and expressed sequence tags, including *MGAT3* (327-fold, $P < 0.001$), fibronectin (*FN1*) (10.1-fold, $P < 0.001$), cholinergic receptor, muscarinic 4 (9.3-fold, $P < 0.001$), and 2′-5′-oligoadenylate synthetase 3 (7.8- fold, $P < 0.001$), and down-regulated (>2-fold) the transcription of 35 genes or ESTs (Table 1).

To confirm these transcriptional differences, we investigated, using quantitative PCR (qPCR), the *MGAT3* responses to Aβ in PBMCs of 18 patients and nine control subjects (Fig. 1). Twelve patients down-regulated *MGAT3* ratio (0.00001–0.99) and six patients (three >80 years old) up-regulated the expression of *MGAT3* ratio. The controls up-regulated the *MGAT3* ratio upon Aβ stimulation with the exception of two subjects >80 years old. The control and AD groups had equal *MGAT3* variances by Levene's test and comparable age distribution; therefore, ANOVA testing

IMMUNOLOGY

Author contributions: M.F. designed research; P.T.L., A.E.-J., L.Z., J.Z., S.D., B.C., J.H., M.M., A.B., and J.C. performed research; M.F., P.T.L., A.E.-J., M.J.R., G.B., J.M.R., J.S., M.M., A.B., P.H., and J.C. analyzed data; and M.F. wrote the paper.

The authors declare no conflict of interest.

This article is a PNAS Direct Submission.

Abbreviations: AD, Alzheimer's disease; Aβ, amyloid-β; TLR, Toll-like receptor; APP, amyloid precursor protein; PBMC, peripheral blood mononuclear cell; IOD, integrated optical density; qPCR, quantitative PCR; CT, cycle threshold; PE, postexposure.

†To whom correspondence should be addressed. E-mail: fiala@mednet.ucla.edu.

This article contains supporting information online at www.pnas.org/cgi/content/full/0701267104/DC1.

Table 1. Transcriptional differences between control subjects' PBMCs exposed to Aβ in comparison to Alzheimer's patients' PBMCs exposed to Aβ

Up-regulated		Down-regulated	
Fold changes	Gene title	Fold changes	Gene title
327.75	β-1,4-MANNOGYL-GLYCOPROTEIN-4-β-*N*-ACETYLGLUCOSAMINYL TRANFERASE	336.57	KIAAD531
126.05	Hypothetical protein LCC285463	156.44	Ramdomized negative control
25.56	Randomized negative control	23.80	X (inactive)-specific transcript
22.79	Smcy homolog Y-linked (mouse)	10.03	NYD-SP28 protein
10.10	Fibronectin 1	9.25	TP53 TARGET GENE 1
9.34	Cholinergic receptor, muscamino 4	6.91	NA
7.81	2¢,5¢-oligoadenytate sythetase 3, 100kDa	4.46	Hypothetical protein FLJ40722
7.49	FERM and POZ domain containing 2	4.24	Killer cell ledin-like receptor subfamily A, member 1
6.47	CD9 antigen (p24)	2.72	KIA0228
5.62	Hypothetical protein LOC 129907	2.69	Chimerin (chimaein) 1
4.71	Alcohol dehydrogenase 4 (class II), pi polypeptide	2.84	Serine/threonine/tyrosine kinase 1
4.65	TBC1 domain family, member 22A	2.91	CONA FLJ25807 fa, don C8R03768
4.31	Aldehyde dehydrogenase 1 family, member A2	2.54	PUTATIVE EMU2
4.28	INTERFERON-INDUCED, HEP C-ASSOCIATED MICROTUBULAR AGGREGATE	2.42	Eukaryotic translation initiation factor 1A pseudogene 1
4.23	Chromosome Y open reading frame 14	2.410	Cysteine-rich secretory protein LCCL domain containing 2
4.07	TAPASIN PRECURSOR (TPSN) (TPN)	2.36	Ceta-like 4 (*Drosophila*)
3.68	VERY HYPOTHETICAL PROTEIN (FRAGMENT)	2.365	T cdl receptor gamma variable 5
3.52	Interferon-induced protein 44-like	2.345	CONA FLJ31407 fs, done NT2NE20001137
3.48	NA	2.345	Midline 2
3.45	NA	2.303	Chromosome 10 open reading frame 24
3.21	Zinc finger protein 415	2.300	COMM domoain containing 5
3.04	LOC440523	2.286	Huntington interacting protein E
3.01	NA	2.253	Mitogen-inactivated protein kinase 2
2.72	MRNA: cDNA DKFZp686B0062	2.150	Ladybird homeobox homolog 2 (*Drosophila*)
2.66	Similar to MGC21861 protein	2.132	Ciaphanous homolog 1 (*Drosophila*)
2.64	Chemokine (C-C motif) ligand 27	2.117	Hypothetical protein LOC283875
2.64	SH3 DOMAIN-BINDING ROTEIN 2 (3BP-2)	2.107	Peroxisomal biogenesis factor 6
3.62	Zona pallucida glycoprotein 4	2.100	Leucine zipper protein FK9314
2.61	NA	2.089	Cancentestis antigen 1B
2.41	Zinc finger protein 577	2.067	Nuclear receptor subfamily 1, group 0, member 2
2.38	Tumor neurosis factor receptor superfamily, member 11a, NFKB activator	2.063	Keratin 6B
2.33	K1AA1948	2.047	AT hock containing transcription factor 1
2.27	Homer homolog 2 (*Drosophila*)	2.048	CYTOKINE-INDUCIBLE SH2-CONTAINING PROTEIN
2.26	Solute carrier family 6 (neurotransmitter transporter betainal GABA, member 12	2.037	Lipopolysaccharide-induced TNF factor
2.248	Regulating synaptic membrane pinocytosis 4	2.034	Signal transducer and activator of transcription 6B

Microarray analysis was performed with RNA isolated from 10 million PBMCs of two patients and two control subjects incubated overnight with Aβ (2 μg/ml). The results indicate RNA in control PBMCs compared with AD. NA, not applicable.

was appropriate. The mean $\log_{10}$ *MGAT3* RNA score (−1.2670) of AD patients was significantly lower in comparison to the mean score of control subjects (+2.190) ($P = 0.025$ by ANOVA). In the 60- to 80-year population sample, the mean log *MGAT3* RNA scores of AD patients (−1.747) and control subjects (+3.77) showed an even greater difference ($P = 0.001$ by ANOVA). Repeat assays of the same patient showed an *MGAT3* ratio of 0.04 in the first sample and *MGAT3* ratios of 0.31 and 0.35 (duplicates) in the second sample 3 months later. In addition, we confirmed by qPCR testing of AD PBMCs transcriptional down-regulation of two other genes noted in the microarray analysis, FN1 and 2′-5′-oligoadenylate synthetase 3.

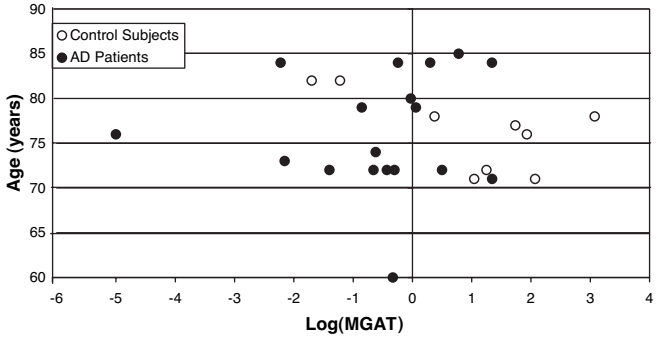

Fig. 1. The relation of the $\log_{10}$ *MGAT3* ratio to age. *MGAT3* ratio (*MGAT3* RNA in PBMCs stimulated with Aβ vs. *MGAT3* RNA in unstimulated PBMCs) was determined in 18 patients and 9 control subjects, as described in *Materials and Methods*.

Relation of Aβ Phagocytosis to Transcription and Translation of *MGAT3*. A review of the results of FITC-Aβ phagocytosis by macrophages of 42 control subjects and 73 patients examined in our prospective studies (2001–2007) showed that macrophages of control subjects usually (≈80%) showed excellent (Fig. 2*A*) or, rarely (≈10%), extremely efficient (Fig. 2*B*) phagocytosis of soluble FITC-Aβ in 24 h. In contrast, macrophages of AD patients displayed either minimal surface uptake of FITC-Aβ (60% of patients) (Fig. 2*C*), no intracellular but strong surface uptake (25%) (Fig. 2*D*), or extremely efficient phagocytosis (as in Fig. 2*B*) (15%). The relationship between *MGAT3* ratio and FITC-Aβ uptake integrated optical density (IOD) per macrophage was analyzed in eight AD patients and four control subjects. The correlation coefficient of *MGAT3* RNA score with IOD was 0.454 ($P < 0.069$) [supporting information (SI) Fig. 7].

To determine directly the effect of *MGAT3* on phagocytosis of FITC-Aβ, we transfected control PBMCs using *MGAT3* siRNA or a control vector or did not transfect them. *MGAT3* siRNA trans-

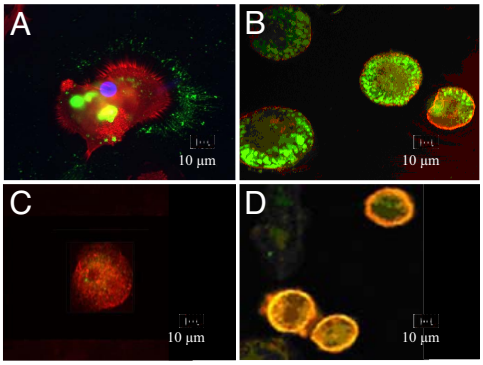

Fig. 2. Phagocytosis of Aβ by macrophages. At 24 h postexposure (PE), control macrophages bind and internalize Aβ into cytoplasmic vesicles. AD macrophages bind Aβ on the surface, either weakly (*C*) or strongly (*D*) but do not internalize it. Phalloidin (red) (*A*), anti-CD68 (red) (*C*), Lysotracker (red) (*B* and *D*), and FITC-Aβ (green) (confocal microscopy).

fection strongly inhibited up-regulation of *MGAT3* ratio (by 99%) and uptake of FITC-Aβ per monocyte (by 85.9%) (Fig. 3). The effects of *MGAT3* siRNA on phagocytosis of FITC-Aβ were complex, including inhibition of monocyte uptake of FITC-Aβ as well as inhibition of monocyte clustering around aggregated Aβ (compare Fig. 3*B a* and *b* with *d*, *e*, *g*, and *h*), and were consistent in two experiments.

The downstream effect of *MGAT3* on phagocytosis may depend upon Toll-like receptors (TLRs), which play a crucial role in the detection of nonself by the innate immune system (23). Therefore, we tested transcription and translation of TLRs in PBMCs.

Transcription of TLRs in Mononuclear Cells of AD Patients and Control Subjects. Using PBMCs of four patients and three control subjects, we examined the transcription of TLRs by PBMCs of patients and controls. Upon Aβ stimulation, AD PBMCs generally down-regulated *TLR* ratios, whereas control PBMCs up-regulated *TLR* ratios. *TLR3*, *TLR4*, *TLR5*, *TLR7*, *TLR8*, *TLR9*, and *TLR10* ratios exhibited the greatest difference between patients and control subjects (Fig. 4). Repeat testing of *TLR* ratios showed comparable results: up-regulation in a control subject and down-regulation in an AD patient.

Previously, we reported that a natural product curcuminoids enhanced phagocytosis of Aβ by macrophages from AD patients in ≈50% of the cases examined (24). We sought to identify the curcuminoid compound that is most transcriptionally and translationally active.

Bisdemethoxycurcumin Is the Most Potent Curcuminoid Compound, Which Enhances Aβ Phagocytosis, *MGAT3*, and *TLR* Transcription and Translation. By an iterative process that was biodirected according to the FITC-Aβ uptake to identify active fractions from curcuminoids, we isolated the most potent immunostimulatory component. The material was purified to near homogeneity and identified by liquid chromatography–MS as bisdesmethoxycurcumin on the basis of its molecular ion and fragmentation pattern. To verify the biological activity of this minor constituent, bisdesmethoxycurcumin was chemically synthesized and tested in the phagocytosis and transcription assays described above. Both the bisdesmethoxycurcumin material isolated by chromatography and the chemically synthesized bisdesmethoxycurcumin material optimally stimulated phagocytosis at 0.1 μM (SI Fig. 8).

To determine whether functional improvement would be accompanied by transcriptional changes, we tested transcriptional up-regulation of *MGAT3* and *TLRs* in PBMCs from AD patients and controls in the presence of Aβ with bisdesmethoxycurcumin (0.1 μM) in comparison to Aβ alone. Bisdemethoxycurcumin improved

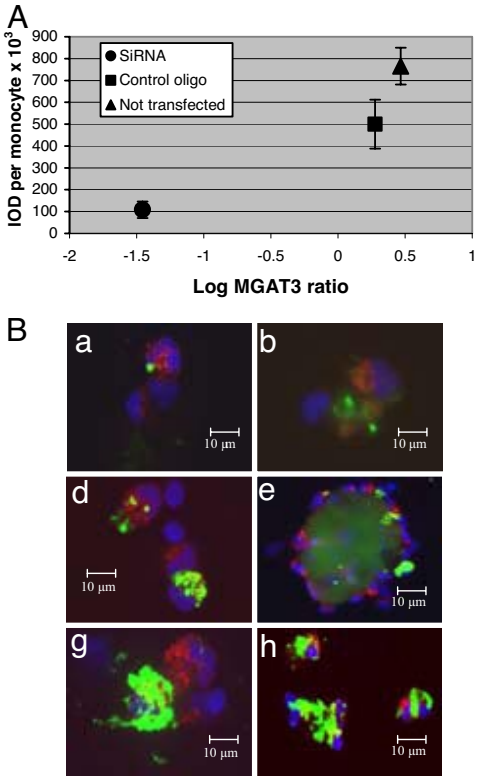

Fig. 3. Transcriptional silencing and inhibition of Aβ phagocytosis using *MGAT3* siRNA. Four million PBMCs were transfected or not transfected as indicated (see *A*). PBMCs (3.9 million) were incubated overnight with or without Aβ (2 μg/ml), and the *MGAT3* ratio was determined as described in *Materials and Methods*. PBMCs (0.1 million) were incubated with FITC-Aβ overnight, spun on a glass slide, stained with anti-CD68/ALEXA 594 and DAPI, and photographed with 40× objective. IODs per monocyte in five replicate fields were determined by ImagePro scanning. (*A*) Relation of MGAT3 ratio to IOD in transfected or not transfected monocytes. (*B*) Fluorescence microscopic pictures of monocytes, which were either transfected with *MGAT3* RNA (*a* and *b*), transfected with control oligo (*d* and *e*), or not transfected (*g* and *h*). Note clustering of monocytes around Aβ in (*d*, *e*, *g*, and *h*) but no clustering in *a* and *b*.

the transcription of *MGAT3* in all four patients (SI Fig. 9). We tested bisdemethoxycurcumin effect on *TLR* transcription in PBMCs of one patient. *TLR* ratios of all 10 TLRs were up-regulated by bisdemethoxycurcumin in this patient (see striped bars in Fig. 4, D vs. D′). To demonstrate the effect of bisdemethoxycurcumin on TLR protein expression, we performed flow cytometry of PBMCs treated with this compound. Aβ and bisdemethoxycurcumin increased the expression of TLR2 (see SI Fig. 10), TLR3, and TLR4 on monocytes.

To determine the intracellular blocks to Aβ phagocytosis, we performed confocal microscopy of macrophages.

Endocytosis and Intracellular Transport of Aβ in Macrophages. In control subjects' macrophages, the intracellular transport of Aβ was rapid, but in most AD patients' macrophages, transport of Aβ progressed slowly or not at all. One and 2 h after exposure of control subjects' macrophages, FITC-Aβ colocalized with the early endosomal marker Rab 5. In contrast, Rab5 staining and colocalization were minimal in AD patients' macrophages (Figs. 5 *A* vs. *F*). The colocalization with the transferrin receptor EEA1 was apparent in control subjects' macrophages but not in AD patients' macrophages (Fig. 5 *B* vs. *G*). In control subjects' macrophages, FITC-Aβ colocalized with the lysosomal marker Lysotracker at each time interval 1, 48, and 72 h after exposure (Fig. 5 *C–E*). In contrast, in AD patients' macrophages, the Aβ cargo bound to the cell surface

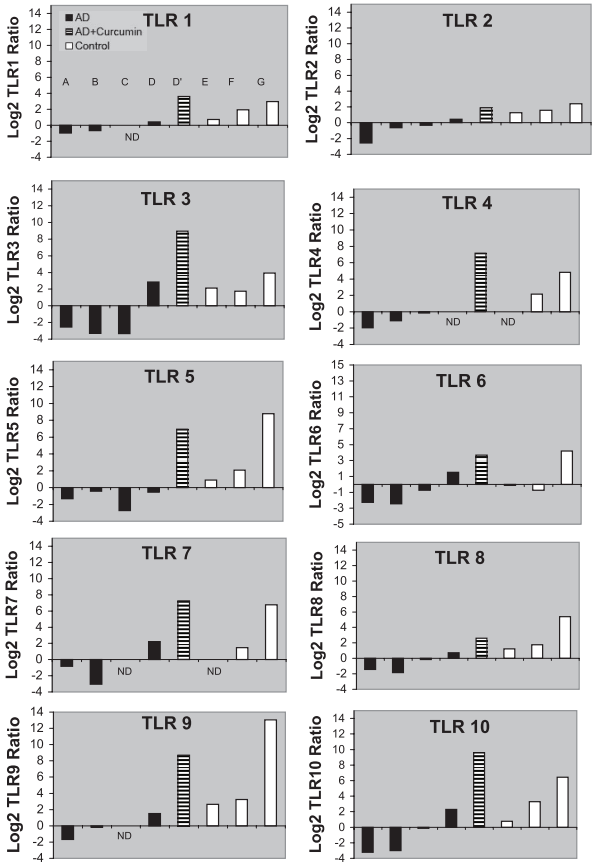

Fig. 4. Up-regulation of *TLR* transcription by Aβ and bisdemethoxycurcumin. Ten million PBMCs each of four AD patients (patients A–D) and three control subjects (E–G) were treated overnight with and without Aβ (patients shown with black bars, controls shown with white bars) or with and without Aβ and bisdemethoxycurcumin (patient D, striped bar). The *TLR* ratio was determined as described in *Materials and Methods.*

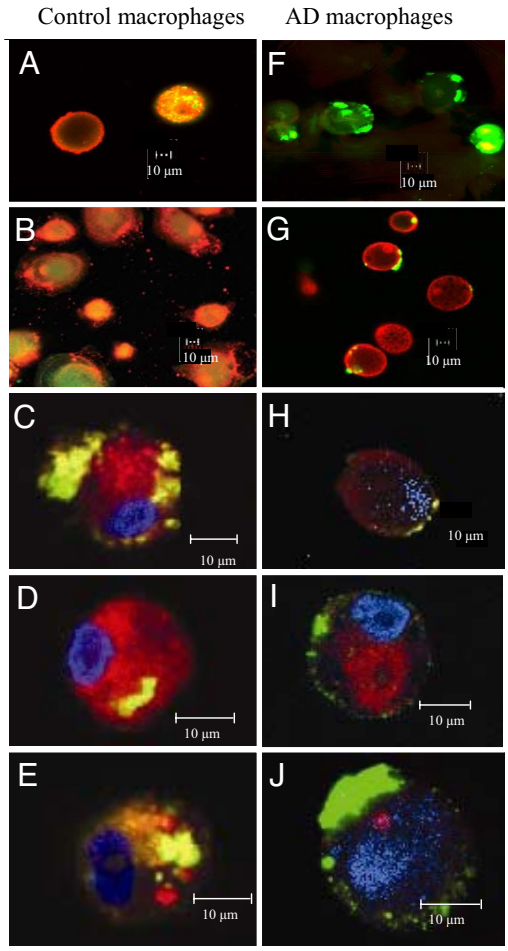

Fig. 5. Trafficking of Aβ in macrophages. (*A–E*) Control macrophages. (*F–J*) AD macrophages. Two hours PE, FITC-Aβ (green) colocalizes with Rab5 (red) in control macrophages (*A*) but minimally in AD macrophages (*F*). Two hours PE, FITC-Aβ (green) colocalizes with EEA1 (red) in control macrophages (*B*) but is surface-bound in AD macrophages (*G*). In control macrophages, FITC-Aβ (green) colocalizes with Lysotracker (red) at 1, 48, and 72 h PE (*C–E*). In AD macrophages, FITC-Aβ is surface-bound at 1, 48, and 72 h PE, and Lysotracker is poorly displayed (*H–J*). *A*, *B*, *F*, and *G* are overlays of 10 sections (40×). *C–E* and *H–J* contain a midsection of a single macrophage. Comparable kinetics of Aβ transport was found in macrophages of four control subjects and three AD patients; macrophages of one AD patient, however, showed normal transport into lysosomes.

but did not progress to lysosomes over a 72-h period, and the lysosomes were poorly expressed (Fig. 5 *H–J*).

Macrophages from both control subjects and patients showed efficient phagocytosis of fluorescently labeled *Escherichia coli* and *Staphylococcus aureus* (SI Fig. 11). Scrambled FITC-Aβ was not taken up by AD or control macrophages.

Uploading of Aβ in Alzheimer's Brain Sections by Control and AD Monocytes. To test the phagocytic ability of monocytes for Aβ species in the brain, we cocultured PBMCs with frozen sections of Alzheimer's brain. In serial experiments, we cocultured PBMCs of four AD patients and four controls with frozen sections of the frontal lobes of three AD patients. The results were consistent, and representative results are shown in the Fig. 6. One-third (12 of 37) of control subjects' monocytes (green) became saturated with Aβ (yellow) in 2 days (Fig. 6*A*) and 100% (35) in 4 days (Fig. 6*B*). In contrast, less than one-quarter (7 of 30) of AD patients' monocytes became saturated with Aβ in 2 days (Fig. 6*E*); in 4 days, the remaining AD patients' monocytes were shrunken and aggregated into approximately nine clusters that stained red and yellow, suggestive of monocyte aggregation and Aβ release (Fig. 6*F*). In brain sections double-stained with anti-CD68 (green)/anti-NeuN (red), monocytes adhered to neurons; whereas control monocytes impinged on neurons (appearing round and yellow) (Fig. 6 *C* and *D*), AD monocytes shriveled (appearing small and green) (Fig. 6 *G* and *H*). The brain section cultures were performed in Iscove's medium with 10% FCS, which excluded the role of antibodies in brain clearance of Aβ.

Discussion

Upon Aβ stimulation, mononuclear cells of AD patients showed defective phagocytosis and transcriptional down-regulation in comparison to control mononuclear cells. The deficiency of innate immunity was highlighted by defective phagocytosis of Aβ *in vitro* as well as poor clearance of AD brain sections by AD monocytes. The most prominent transcriptional defect of AD PBMCs involved down-regulation of *MGAT3* transcription upon Aβ stimulation. MGAT3 may be a key molecule in phagocytosis of Aβ, because silencing its transcription inhibited Aβ phagocytic function of control monocytes. The product of the *MGAT3* gene is *N*-acetylglucosaminyltransferase III (GlcNAc-TIII) (25, 26), which transfers the bisecting *N*-acetylglucosamine to the core mannose of complex *N*-glycans (25, 27). GlcNAc-TIII stops further processing and elongation of *N*-glycans (28). GlcNAc-TIII modulates cell

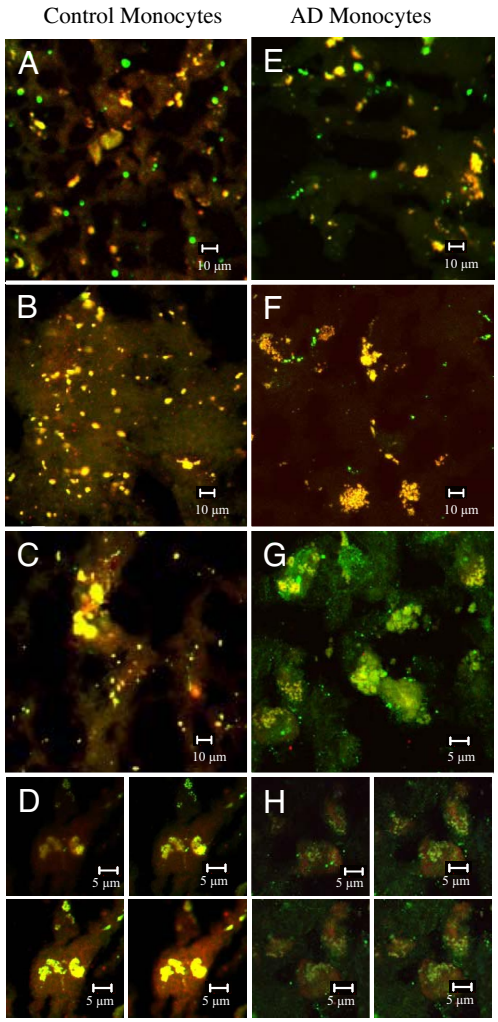

Fig. 6. Migration of monocytes into the frontal lobe sections of AD brain and uploading of Aβ. (*A–D*) Control monocytes. (*C* and *D*) AD monocytes. (*A*) Two days after coculture of AD brain section with control PBMCs (subject A), 25 monocytes stain green and 12 stain yellow. (*B*) At 4 days after coculture (subject A), all 35 monocytes stain yellow. (*C*) Coculture with control PBMCs (subject B), yellow monocytes aggregated on neurons (red). (*D*) Coculture with control PBMCs (subject C) shows green to yellow monocytes apposed and indenting neurons (red) (*z* sections from top to bottom). (*E*) At 2 days after coculture with PBMCs of AD patient (patient A), 23 AD monocytes stain green, and 7 stain yellow but appear shrunken. (*F*) At 4 days after coculture (patient A), there are approximately nine clusters of aggregated shrunken cells staining yellow/red (suggesting that these monocytes uploaded and released Aβ). (*G*) Coculture (patient B) shows approximately eight clusters of green/yellow shrunken monocytes. (*H*) Coculture with AD PBMCs (patient C) shows shrunken green monocytes impinging on neurons. *A–C* and *E–F* are stained with anti-Aβ/ALEXA594 and CD68/ALEXA488. *C*, *D*, *G*, and *H* are stained with anti-NeuN/ALEXA594 and CD68/ALEXA488.

interactions, such as decreased binding of the erythroagglutinin from *Phaseolus vulgaris* to Chinese hamster ovary cells (29). Animals with truncated inactive GlcNAc-TIII show neurological dysfunction (30). GlcNAc-TIII potentiates β1 integrin-mediated neuritogenesis (31). α2β1 and αVβ1 integrins may recognize and be activated by amyloidogenic proteins (32) and thus could be the targets of GnT-III. The overexpression of GlcNAc-TIII protects against hydrogen peroxide-induced apoptosis (33). We speculate that, because AD macrophages are more susceptible to apoptosis by Aβ in comparison to control macrophages (26), they might be stabilized by *MGAT3* overexpression. Furthermore, altered glycosylation noted in AD (14) could be related to transcriptional dysregulation of GlcNAc-TIII.

Abnormal processing of APP assumes an important role in AD, as suggested by misdirection of APP into Aβ-generating compartments when SORL1 is underexpressed (13). Neurons of patients with Down's syndrome (34) display abnormal lysosomes (35) and defective hydrolases. Abnormalities of lysosomal degradation are also noted in patients with presenilin 1 mutation and sporadic AD patients (36).

TLRs are crucial for macrophage function. We found a striking difference in *TLR* mRNA levels between control and AD PBMCs stimulated with Aβ, where AD cells expressed lower levels of all *TLR*s tested. *TLR3*, *TLR4*, *TLR5*, *TLR7*, *TLR8*, *TLR9*, and *TLR10* exhibited the greatest difference. TLRs are pattern recognition receptors found on many cells types, including cells of the innate immune system, and they recognize conserved pathogen associated molecular patterns. Activation of a TLR results in many functional outcomes, including the enhancement of apoptosis, secretion of inflammatory cytokines, and direct antimicrobial activity (37). The lower expression levels of TLRs on AD macrophages may be indicative of more global innate immune defects beyond Aβ phagocytosis. The innate and adaptive immune systems of AD patients appear to be in various states of disharmony. We previously observed that the intracellular levels of both T_{H1}- (IL-12 and IFN-γ) and T_{H2}-(IL-10) cytokines in mononuclear cells are significantly higher in AD patients in comparison to control subjects (26). Discrepant serum and cerebrospinal fluid levels of cytokines in different studies [either increased or significantly diminished levels (38)] also suggest that the coordination between adaptive and innate immune systems may change with the stage of the disease.

The immunotherapeutic Aβ vaccine strategy was designed in animal models to increase Aβ clearance by microglia through Fcγ receptor phagocytosis (39). However, the clearance of human AD brain may depend on bone marrow-derived macrophages (4) rather than resident brain microglia. Furthermore, antibody opsonization could increase inflammation (40). Therefore, the enhancement of Aβ phagocytosis (24) and gene transcription in macrophages using the natural substance curcuminoids may have important applications to the immunotherapy of AD. However, it is not clear whether the blood levels achieved after oral administration of curcuminoids would be therapeutic. Here we have isolated bisdemethoxycurcumin as the most immunoenhancing chemical in curcuminoids, which also increased *Mgat3* and *TLR* transcription. Our results show that bisdemethoxycurcumin is active at 0.1 μM *in vitro*, and such blood level could be achieved by infusion. Therefore, our results may provide an entirely different direction to therapeutic opportunities in AD through the repair of the functional and transcriptional deficits of AD macrophages by curcuminoids.

Materials and Methods

Patients and Controls. A total of 73 patients (mean age 74.4 + 8.7 years, mean minimental score examination 22.6 + 3.7) with a diagnosis of probable AD established by the National Institute of Neurological and Communication Disorders and Stroke/Alzheimer's Disease and Related Disorders Association criteria (41) were recruited into the study since 2001 through the University of California, Los Angeles (UCLA), Alzheimer's Disease Research Center under a UCLA Institutional Review Board-approved protocol. In addition, 42 control subjects (mean age 69.4 + 9.4 years) were recruited from UCLA personnel and families of patients.

PBMCs and Macrophage Cultures. PBMCs were isolated by the Ficoll–Hypaque gradient technique from venous blood (20–30 ml) and were differentiated into adherent macrophages (7–14 days) as described (42). See *SI Text* for details.

Phagocytosis Assay, Fluorescence, and Confocal Microscopy. Testing of FITC-Aβ (1–42) phagocytosis was performed as described (42). See *SI Text* for details.

Microarray Hybridization. Hybridization to the Operon Human Genome Oligo Set Version 3.0 (Operon, Huntsville, AL) was performed at the Duke Microarray Facility. ANOVA was performed by using the software VizX GeneSifter. Genes with $P < 0.05$ and a fold change of at least 3- fold were selected for further testing by qPCR. See *SI Text* for details.

qPCR. The expression levels of the genes of interest were tested by qPCR on an Opticon real-time PCR detector (BioRad, Hercules, CA) as described (44). The relative quantities of the genes tested were calculated against h36B4 as a reference using the ΔΔCT (CT, cycle threshold) formula, as described (44). To account for the variable baseline between subjects, the change in *MGAT3* levels due to Aβ stimulation was calculated as the ratio (*MGAT3* RNA in PBMCs stimulated with Aβ/*MGAT3* RNA in unstimulated PBMCs). See *SI Text* for details.

siRNA Transfection. We transfected PBMCs using the Amaxa Nucleofection system and the primary human monocyte transfection kit (Amaxa, Cologne, Germany) by using either MGAT3 siRNA [Dharmacon (Lafayette, CO) NM_002409] or a nonspecific control oligo (Dharmacon D-001810-01-05), or were not transfected. See *SI Text* for details.

Flow Cytometry of TLRs. PBMCs were either untreated or treated with FITC-Aβ (2 μg/ml) ± bisdemethoxycurcumin (0.1 μM), stained with PE-anti-TLR2 (BioLegend, San Diego, CA), PE-anti-TLR3 (BioLegend), or PE-anti-TLR4 (eBioscience, San Diego, CA) and FITC-anti-CD14 (BD Pharmingen, San Diego, CA), and examined by using BD FACScan Analytic Flow cytometer. See *SI Text* for additional information.

Clearance of Aβ in Brain Sections. Frozen sections of frontal lobe tissue were incubated with PBMCs and stained by indirect immunofluorescence using antibodies to CD68 and Aβ(1–42) and ALEXA488- and 594-conjugated secondary antibodies. See *SI Text* for additional information.

Chromatography of Curcuminoids. Curcuminoids were chromatographed on a silica gel column (Silica Gel 60 A Partisil PK6F; Whatman, Maidstone, U.K.). The active fraction was further separated with preparative silica gel TLC. The fraction having an R_f value of 0.49 showed the greatest activity and was analyzed on a reversed-phase HPLC system [Waters (Milford, MA) 2525 Binary Gradient System] with a Waters 2487 dual wavelength UV-vis detector and a Waters Micromass ZQ mass detector. The HPLC column (C-18 19 × 50 mm column; Thompson Instruments, Clear Brook, VA) was eluted with a gradient starting from acetonitrile: water (5:95, vol:vol) to acetonitrile:water (95:5, vol:vol) at a rate of 1.5 ml/min over 5 min with UV detection set at 220 nm. A prominent material eluted with a retention time of 2.17 min and was ≈90% pure on the basis of total ion current. The HPLC peak eluting at 2.17 min showed a prominent ion of *m/z* 308. A larger ion at *m/z* 290 (arising from loss of water) was also observed. A subsequent electrospray mass spectrometry experiment also showed the anticipated *m/z* 309 and *m/z* 291 for the [M + 1] ions. The most active fraction corresponded to bisdemethoxycurcumin, which was also chemically synthesized and successfully tested (SI Fig. 7). See *SI Text* for additional information.

We thank N. Taniguchi and P. Stanley for a discussion of the possible role of MGAT3 in macrophages. Milad Alam; Pooya Banapour; Eric Tse; Allison Chin; Ben Goldenson; Nichole Stevens; Barbara Carter, R.N.; and Edmond Teng, M.D. provided invaluable assistance with this study. This study was supported in part by the grant "Blood–Brain Barrier in Alzheimer's Disease" from the Alzheimer's Disease Association (to M.F.) and the Alzheimer's Drug Discovery Foundation (to J.C.). Microbial Pathogenesis Training Grant 2-T32-AI-07323 supports P.L. We are grateful for support by Herman and Lisbeth Rosenfeld (to M.F.) and Ms. Jean Young (to J.C.). We thank H.Vinters (University of California Brain Bank, Los Angeles, CA) and G. Perry (Department of Pathology, Case Western Reserve University, Cleveland, OH) for providing brain tissues of AD patients. The Duke Microarray Facility performed microarray probe preparation and hybridization.

1. Luhrs T, Ritter C, Adrian M, Riek-Loher D, Bohrmann B, Dobeli H, Schubert D, Riek R (2005) *Proc Natl Acad Sci USA* 102:17342–17347.
2. Bitan G, Fradinger EA, Spring SM, Teplow DB (2005) *Amyloid* 12:88–95.
3. Hardy J, Selkoe DJ (2002) *Science* 297:353–356.
4. Fiala M, Liu QN, Sayre J, Pop V, Brahmandam V, Graves MC, Vinters HV (2002) *Eur J Clin Invest* 32:360–371.
5. Akiyama H, Barger S, Barnum S, Bradt B, Bauer J, Cole GM, Cooper NR, Eikelenboom P, Emmerling M, Fiebich BL, *et al.* (2000) *Neurobiol Aging* 21:383–421.
6. Streit WJ, Mrak RE, Griffin WS (2004) *J Neuroinflamm* 1:14.
7. D'Andrea MR, Cole GM, Ard MD (2004) *Neurobiol Aging* 25:675–683.
8. Walker DG, Link J, Lue LF, Dalsing-Hernandez JE, Boyes BE (2006) *J Leukocyte Biol* 79:596–610.
9. Simard AR, Soulet D, Gowing G, Julien JP, Rivest S (2006) *Neuron* 49:489–502.
10. Forman MS, Trojanowski JQ, Lee VM (2004) *Nat Med* 10:1055–1063.
11. Mahley RW, Weisgraber KH, Huang Y (2006) *Proc Natl Acad Sci USA* 103:5644–5651.
12. Sadowski MJ, Pankiewicz J, Scholtzova H, Mehta PD, Prelli F, Quartermain D, Wisniewski T (2006) *Proc Natl Acad Sci USA* 103:18787–18792.
13. Rogaeva E, Meng Y, Lee JH, Gu Y, Kawarai T, Zou F, Katayama T, Baldwin CT, Cheng R, Hasegawa H, *et al.* (2007) *Nat Genet* 39:168–177.
14. Botella-Lopez A, Burgaya F, Gavin R, Garcia-Ayllon MS, Gomez-Tortosa E, Pena-Casanova J, Urena JM, Del Rio JA, Blesa R, *et al.* (2006) *Proc Natl Acad Sci USA* 103:5573–5578.
15. Mrak RE, Griffin WS (2000) *J Neuropathol Exp Neurol* 59:471–476.
16. Licastro F, Porcellini E, Caruso C, Lio D, Corder EH (2006) *Neurobiol Aging*, doi.10.1016/j.neurobiolaging.2006.07.007.
17. Cutler RG, Kelly J, Storie K, Pedersen WA, Tammara A, Hatanpaa K, Troncoso JC, Mattson MP (2004) *Proc Natl Acad Sci USA* 101:2070–2075.
18. Mattson MP (2006) *Antioxid Redox Signal* 8:1997–2006.
19. Jordan-Sciutto K, Rhodes J, Bowser R (2001) *Mech Ageing Dev* 123:11–20.
20. Wang Y, Xie WY, He Y, Wang M, Yang YR, Zhang Y, Yin DM, Jordan-Sciutto KL, Han JS, Wang Y (2006) *Exp Neurol* 202:313–323.
21. Bredesen DE, Rao RV, Mehlen P (2006) *Nature* 443:796–802.
22. Selkoe DJ (2004) *Ann Intern Med* 140:627–638.
23. Takeda K, Kaisho T, Akira S (2003) *Annu Rev Immunol* 21:335–376.
24. Zhang L, Fiala M, Cashman J, Sayre J, Espinosa-Jeffrey A, Mahanian M, Zaghi J, V, B., Graves M, Bernard G, Rosenthal M (2006) *J Alzheimers Dis* 10:1–7.
25. Nishikawa A, Ihara Y, Hatakeyama M, Kangawa K, Taniguchi N (1992) *J Biol Chem* 267:18199–18204.
26. Ihara Y, Nishikawa A, Tohma T, Soejima H, Niikawa N, Taniguchi N (1993) *J Biochem (Tokyo)* 113:692–698.
27. Narasimhan S (1982) *J Biol Chem* 257:10235–10242.
28. Taniguchi N, Miyoshi E, Ko JH, Ikeda Y, Ihara Y (1999) *Biochim Biophys Acta* 1455:287–300.
29. Campbell C, Stanley P (1984) *J Biol Chem* 259:13370–13378.
30. Bhattacharyya R, Bhaumik M, Raju TS, Stanley P (2002) *J Biol Chem* 277:26300–26309.
31. Shigeta M, Shibukawa Y, Ihara H, Miyoshi E, Taniguchi N, Gu J (2006) *Glycobiology* 16:564–571.
32. Wright S, Malinin NL, Powell KA, Yednock T, Rydel RE, Griswold-Prenner I (2007) *Neurobiol Aging* 28:226–237.
33. Shibukawa Y, Takahashi M, Laffont I, Honke K, Taniguchi N (2003) *J Biol Chem* 278:3197–3203.
34. Cataldo AM, Hamilton DJ, Barnett JL, Paskevich PA, Nixon RA (1996) *J Neurosci* 16:186–199.
35. Cataldo AM, Hamilton DJ, Nixon RA (1994) *Brain Res* 640:68–80.
36. Cataldo A, Rebeck GW, Ghetri B, Hulette C, Lippa C, Van Broeckhoven C, van Duijn C, Cras P, Bogdanovic N, Bird T, *et al.* (2001) *Ann Neurol* 50:661–665.
37. Krutzik SR, Ochoa MT, Sieling PA, Uematsu S, Ng YW, Legaspi A, Liu PT, Cole ST, Godowski PJ, Maeda Y, *et al.* (2003) *Nat Med* 9:525–532.
38. Richartz E, Stransky E, Batra A, Simon P, Lewczuk P, Buchkremer G, Bartels M, Schott K (2005) *J Psychiatr Res* 39:535–543.
39. Bard F, Cannon C, Barbour R, Burke RL, Games D, Grajeda H, Guido T, Hu K, Huang J, Johnson-Wood K, *et al.*(2000) *Nat Med* 6:916–919.
40. Lue LF, Walker DG (2002) *J Neurosci Res* 70:599–610.
41. McKhann G, Drachman D, Folstein M, Katzman R, Price D, Stadlan EM (1984) *Neurology* 34:939–944.
42. Fiala M, Lin J, Ringman J, Kermani-Arab V, Tsao G, Patel A, Lossinsky AS, Graves MC, Gustavson A, Sayre J, *et al.* (2005) *J Alzheimers Dis* 7:221–232; discussion 255–262.
43. Renn CN, Sanchez DJ, Ochoa MT, Legaspi AJ, Oh CK, Liu PT, Krutzik SR, Sieling PA, Cheng G, Modlin RL (2006) *J Immunol* 177:298–305.
44. Monney L, Sabatos CA, Gaglia JL, Ryu A, Waldner H, Chernova T, Manning S, Greenfield EA, Coyle AJ, Sobel RA, *et al.* (2002) *Nature* 415:536–541.